Trajectory Generation for Autonomous Mobile Robots

Chapter · February 2014

DOI: 10.1007/978-981-4585-36-1_6

1 author:

Vu Trieu Minh
Tallinn University of Technology
69 PUBLICATIONS **451** CITATIONS

Trajectory Generation for Autonomous Mobile Robots

Vu Trieu Minh

Abstract This chapter presents the generation of car-like autonomous mobile robots/vehicles tracking trajectory with three different methods comprising of flatness, polynomial and symmetric polynomial equations subject to constraints. Kinematic models for each method are presented with all necessary controlled variables including position, body angle, steer angle and their velocities. The control systems for this model are designed based on fuzzy/neural networks. Simulations are analyzed and compared for each method. Studies of this chapter can be used to develop a real-time control system for auto-driving and/or auto-parking vehicles.

Keywords Trajectory generation · Autonomous mobile robot · Nonholonomic · Flatness · Polynomial

1 Introduction

This chapter studies the problem associated with trajectory generation for car-like autonomous mobile robots moving from an initial point to any final point subject to constraints. This study can be used to develop a real-time control system for autonomous ground vehicles which can track on any feasible paths from the global positioning system (GPS) maps or/and from unmanned aerial vehicle (UAV) images. This system can be applied to autonomous unmanned ground vehicles (on road or off road), and auto-parking, auto-driving systems. The vehicles can perform intelligent motion without requiring a guidance command or remote teleoperation.The main idea of this chapter is to propose a system which can

V. T. Minh (✉)
Mechanosystem—Department of Mechatronics, Tallinn University of Technology, Tallinn, Estonia
e-mail: vutrieuminh@yahoo.com

Z. H. Khan et al. (eds.), *Computational Intelligence for Decision Support in Cyber-Physical Systems*, Studies in Computational Intelligence 540,
DOI: 10.1007/978-981-4585-36-1_6,

automatically generate an optimally feasible trajectory, and then, control the autonomous vehicles/robots to track exactly on this path from any given starting point to any desired destination point from a map subject to the vehicle's physical constraints due to obstacles, speed, steer angle, etc.

In order to deal with the constrained trajectory generation problem, all constraints from a real vehicle must be included into the equations such as the size, position, body angle, steer angle and their velocities. Looking at the current research articles on this topic, there are very few of them dealing with real automotive engineering constraints. Basic introduction on flatness, nonholonomic, and nonlinear systems can be read from Levine [7], where the fundamental motion planning of a vehicle is presented. Parking simulation of 2-trailer vehicle is also demonstrated but without constraints of steer angle and steer angular velocity. The problem of trajectory generation for nonholonomic system is also well considered by Dong and Guo [3], where two trajectory generation methods are proposed. The control inputs are the second order polynomial equations. By integrating those control inputs, coefficients for the second order polynomial equations are found. However, this article is lacking constraints analysis on the vehicle velocity as well as the steer angle.

Optimal control based on cell mapping techniques for a car-like robot is studied by Gomez [4] subject to the energy-optimal constraint and based on bang-bang control theory. This article shows a simulation of a wheeled mobile robot moving on a path with the steering angle velocity control. However, the article does not mention the algorithms for generating the vehicle trajectory. Several other research articles on optimal trajectories and control of autonomous mobile robots can be seen e.g. by Wang et al. [13], Werling et al. [14], Kanjanawanishkul et al. [5], and Klancar [6]. However, most of those studies are based on the real traffic flow and the control algorithms are to perform the maneuver tasks such as lane-changing, merging, distance-keeping, velocity-keeping, stopping and collision avoidance etc.

This book chapter, therefore, concentrates on the applicable mathematic algorithms to generate optimal trajectories from any start point to any destination point subject to feasible vehicle constraints. This book chapter is the continuation of the previous research article on vehicle sideslip model and estimation by Minh [8]. Nonlinear computational schemes for the nonlinear systems are discussed from Minh and Nitin [11] and Minh and Fakhruldin [10]. Although, the holonomous-dynamical trajectories generation is not new, recent research articles have tried to develop those trajectories in different applications: Trajectory for autonomous ground vehicles based on Bezier curves operating under waypoints and corridor constraints can be referred to Minh [9] and Choi et al. [1]. A real-time trajectory generation for car-like vehicles navigating dynamic environments is discussed in Delsart et al. [2]. A recent paper on trajectory generation of model-based IMM tracking for safe driving in intersection scenario is described in Zhou et al. [15] to reduce traffic accidents at intersections. Another related work on dynamic trajectory generation for wheeled robots is discussed in Missura and Behnke [12] where a dynamic motion of wheeled robots can be determined in real-time onboard.

This chapter introduces three conventional holonomous trajectories generation algorithms (flatness, polynomial and symmetric) subject to steering angle constraint for autonomous mobile robots. Performances of these three algorithms are compared. Data taken from the simulation of the vehicle's longitudinal velocity and its steering angular velocity will be used to develop the control algorithms for the mobile robot tracking on those trajectories in the next part of this chapter. The outline of this chapter is as follows: Sect. 2 describes the kinematic model for a mobile robot; Sect. 3 presents the flatness method for the mobile robot trajectory generation; Sect. 4 discusses the trajectory generation subject to steer angle constraint; Sect. 5 introduces the polynomial method for trajectory generation; Sect. 6 develops the symmetric polynomial method; Sect. 7 analyses the performances of the three methods and finally the conclusion is drawn in Sect. 8.

2 Kinematic Model of a Mobile Robot

The constraints for the mobile robot model are based on the assumption that the wheels are rolling without slipping and the steering angle is simplified as a single wheel at the midpoint of the two front wheels. Then, a kinematic model of the mobile robot shown in Fig. 1 can be drawn as under.

The kinematic model of a forward rear-wheel driving mobile robotis written as:

$$\begin{bmatrix} \dot{x} \\ \dot{y} \\ \dot{\theta} \\ \dot{\varphi} \end{bmatrix} = \begin{bmatrix} \cos\theta \\ \sin\theta \\ \frac{\tan\varphi}{l} \\ 0 \end{bmatrix} r v_1 + \begin{bmatrix} 0 \\ 0 \\ 0 \\ 1 \end{bmatrix} v_2 \tag{1}$$

where $X = [x, y, \theta, \varphi]'$ is the system state variables, (x, y) are the Cartesian coordinates of the middle point of the rear wheel axis, θ is the angle of the vehicle body to the x-axis, φ is the steering angle, l is the vehicle wheel base, r is the wheel radius, v_1 is the angular velocity of the rear wheel, and v_2 is the angular steering velocity. Given the initial state $X(0) = [x_0, y_0, \theta_0, \varphi_0]'$ at time $t = 0$ and the final state $X(T) = [x_T, y_T, \theta_T, \varphi_T]'$ at time $t = T$, the paper generates a feasible trajectory for this vehicle. Similarly, the model for a forward front-wheel driving vehicle is presented as:

$$\begin{bmatrix} \dot{x} \\ \dot{y} \\ \dot{\theta} \\ \dot{\varphi} \end{bmatrix} = \begin{bmatrix} \cos\theta\cos\varphi \\ \sin\theta\cos\varphi \\ \frac{\tan\varphi}{l} \\ 0 \end{bmatrix} r v_1 + \begin{bmatrix} 0 \\ 0 \\ 0 \\ 1 \end{bmatrix} v_2 \tag{2}$$

For a vehicle moving in a reverse direction (backing), the velocity, v_1 of this vehicle is assigned a negative value. Then, the general kinematic model in (1) is changed to:

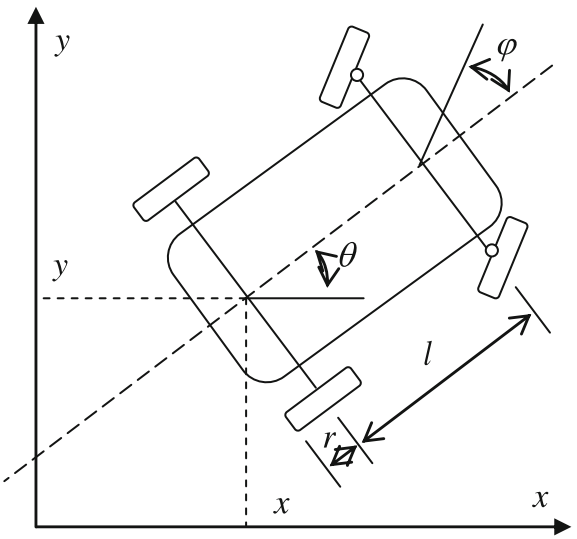

Fig. 1 A simplified mobile robot model

$$\begin{bmatrix} \dot{x} \\ \dot{y} \\ \dot{\theta} \\ \dot{\varphi} \end{bmatrix} = -\begin{bmatrix} \cos\theta \\ \sin\theta \\ \frac{\tan\varphi}{l} \\ 0 \end{bmatrix} rv_1 + \begin{bmatrix} 0 \\ 0 \\ 0 \\ 1 \end{bmatrix} v_2 \tag{3}$$

From the above three fundamental equations, flatness equations for the moving vehicle are investigated in the next section.

3 Flatness Trajectory Generation

From Fig. 1, the vehicle angular velocity can be calculated as:

$$rv_1 = \sqrt{\dot{x}^2 + \dot{y}^2} \Rightarrow v_1 = \frac{\sqrt{\dot{x}^2 + \dot{y}^2}}{r} \tag{4}$$

Transformation from Eq. (1), the vehicle body angle is:

$$\frac{\dot{y}}{\dot{x}} = \frac{rv_1 \sin\theta}{rv_1 \cos\theta} = \tan\theta \Rightarrow \theta = \arctan\left(\frac{\dot{y}}{\dot{x}}\right) \tag{5}$$

From the derivative of the above trigonometric relationship for body angular velocity (θ), its derivative $\dot{\theta}$, is achieved as follows:

$$\dot{\theta} = \frac{\ddot{y}\dot{x} - \ddot{x}\dot{y}}{\dot{x}^2} \frac{1}{\left(\frac{\dot{y}}{\dot{x}}\right)^2 + 1} = \frac{\ddot{y}\dot{x} - \ddot{x}\dot{y}}{\dot{x}^2 + \dot{y}^2} = \frac{\tan\ \varphi}{l} r v_1 \Rightarrow \varphi = \arctan\left(l \frac{\ddot{y}\dot{x} - \ddot{x}\dot{y}}{r(\dot{x}^2 + \dot{y}^2)^{\frac{3}{2}}}\right) \tag{6}$$

Therefore, θ and φ can be directly calculated from other variables, i.e. $\dot{x}$, $\ddot{x}$, and $\dot{y}$, $\ddot{y}$. And it means that the above system is flat in Levine [7]. Thus, all state and input variables can be presented by the flat outputs x and y. The boundary conditions for the outputs x and y are:

$$\begin{aligned} \frac{\partial y}{\partial x} = \tan\ \theta \Rightarrow \frac{\partial^2 y}{\partial x} = \dot{\theta} \frac{1}{\cos^2\ \theta} = \frac{\tan\ \varphi}{l} r v_1 \frac{1}{\cos^2\ \theta} = \frac{\tan\ \varphi}{l} \frac{\partial x}{\cos\ \theta} \frac{1}{\cos^2\ \theta} \\ \Rightarrow \frac{\partial^2 y}{\partial x^2} = \frac{\tan\ \varphi}{l \cos^3\ \theta} \end{aligned} \tag{7}$$

For $x(t)$, the initial state at time, $t\ = 0$, to the final state at time, $t\ = T$:

$$x(0) = x_0 \Rightarrow x(T) = x_T \tag{8}$$

The initial state for $y(t) = y(0)$ is given as:

$$y(0) = y_0 = \tan\ \theta_0 \Rightarrow \frac{\partial^2 y}{\partial x^2}|_{t=0} = \frac{\tan\ \varphi_0}{l \cos^3\ \theta_0} \tag{9}$$

and the final state for $y(t) = y(T)$:

$$y(T) = y_T = \tan\ \theta_T \Rightarrow \frac{\partial^2 y}{\partial x^2}|_{t=T} = \frac{\tan\ \varphi_T}{l \cos^3\ \theta_T} \tag{10}$$

From the initial state $(x_0, y_0, \theta_0, \varphi_0)$ at the time $t = 0$ to the final state $(x_T, y_T, \theta_T, \varphi_T)$, and under a real condition that $|\dot{x}(t)| \geq \varepsilon > 0$. If it is assumed that, $\varepsilon = \frac{|x_T - x_0|}{2T} > 0$, the trajectory of $x(t)$ can be selected freely as:

$$x(t) = \left(\frac{T - t}{T}\right) x_0 + \frac{t}{T} x_T + |x_T - x_0| \frac{t(t - T)}{2T^2} \tag{11}$$

And the trajectory of $y(t)$ can be selected as:

$$y(t) = y_0 + t\alpha_1 \tan\ \theta_0 + t^2 \frac{\alpha_2 \tan\ \varphi_0}{2l \cos^3\ \theta_0} + t^3 b_1 + t^4 b_2 + t^5 b_3 \tag{12}$$

where, $\alpha_1 = \frac{2(x_T - x_0) - |x_T - x_0|}{2T}$, $\alpha_2 = \frac{|x_T - x_0|}{T^2}$, and $\alpha_3 = \frac{2(x_T - x_0) + |x_T - x_0|}{2T}$;

and $b = [b_1, b_2, b_3]' = A^{-1}c$ with:

$$A = \begin{bmatrix} T^3 & T^4 & T^5 \\ 3T^2 & 4T^3 & 5T^4 \\ 6T & 12T^2 & 20T^3 \end{bmatrix} \text{ and } c = \begin{bmatrix} y_T - y_0 - T\alpha_1 \tan\ \theta_0 - T^2 \frac{\alpha_2 \tan\ \varphi_0}{2l \cos^3\ \theta_0} \\ \alpha_3 \tan \theta_T - \alpha_1 \tan\ \theta_0 - T \frac{\alpha_2 \tan\ \varphi_0}{l \cos^3\ \theta_0} \\ \frac{\alpha_2 \tan\ \varphi_T}{l \cos^3\ \theta_T} - \frac{\alpha_2 \tan\ \varphi_0}{l \cos^3\ \theta_0} \end{bmatrix}.$$

From Eq. (10),

$$\theta = \arctan\left(\frac{2T^2\left(\alpha_1 \tan\,\theta_0 + \frac{\alpha_2 \tan\,\varphi_0}{l\cos^3\,\theta_0}t + 3b_1t^2 + 4b_2t^3 + 5b_3t^4\right)}{(2T(x_T - x_0) - T|x_T - x_0| + 2|x_T - x_0|t)}\right) \tag{13}$$

and from Eq. (5),

$$\begin{aligned}\varphi &= \arctan\left(\frac{\partial^2(y) l\cos^3\,\theta}{\partial x^2}\right) \\ &= \arctan\left(\frac{\left(\frac{\alpha_2 \tan\,\varphi_0}{l\cos^3\,\theta_0} + 6b_1t + 12b_2t^2 + 20b_3t^3\right)(2T^2)^2 l\cos^3\,\theta}{(2T(x_T - x_0) - T|x_T - x_0| + 2|x_T - x_0|t)^2}\right)\end{aligned} \tag{14}$$

The angular velocity of the vehicle in Eq. (1) can be calculated from (11) and (12) for y:

$$\dot{y}(t) = \left(\alpha_1 \tan\,\theta_0 + \frac{\alpha_2 \tan\,\varphi_0}{l\cos^3\,\theta_0}t + 3b_1t^2 + 4b_2t^3 + 5b_3t^4\right) \tag{15}$$

and then,

$$\ddot{y}(t) = \left(\frac{\alpha_2 \tan\,\varphi_0}{l\cos^3\,\theta_0} + 6b_1t + 12b_2t^2 + 20b_3t^3\right) \tag{16}$$

And for x:

$$\dot{x}(t) = \left(\frac{(2T(x_T - x_0) - T|x_T - x_0| + 2|x_T - x_0|t)}{2T^2}\right) \tag{17}$$

And then,

$$\ddot{x}(t) = \left(\frac{|x_T - x_0|}{T^2}\right) \tag{18}$$

The absolute vehicle velocity can be calculated from Eqs. (15) to (18):

$$v_1(t) = \frac{\sqrt{\dot{x}^2 + \dot{y}^2}}{r} \tag{19}$$

or with another method to calculate $v_1(t)$ is $v_1(t) = \frac{\dot{x}(t)\cos\,\theta}{r} + \frac{\dot{y}(t)\sin\,\theta}{r}$, then:

$$\begin{aligned}v_1(t) = &\left(\frac{(2T(x_T - x_0) - T|x_T - x_0| + 2|x_T - x_0|t)}{2rT^2}\right)\cos\,\theta \\ &+ \left(\frac{\left(\alpha_1 \tan\,\theta_0 + \frac{\alpha_2 \tan\,\varphi_0}{l\cos^3\,\theta_0} + 3b_1t^2 + 4b_2t^3 + 5b_3t^4\right)\sin\,\theta}{r}\right)\end{aligned} \tag{20}$$

To calculate $\dot{\theta}$ from Eq. (6):

$$\dot{\theta} = \frac{\ddot{y}\dot{x} - \ddot{x}\dot{y}}{\dot{x}^2 + \dot{y}^2} = \frac{\tan\,\varphi}{l} r v_1 \tag{21}$$

To calculate $v_2(t) = \dot{\varphi}$, from Eq. (14), if $\varphi = \arctan(X)$, then,

$$\begin{aligned} \dot{\varphi} &= \dot{X}\left(\frac{1}{1+X^2}\right) \text{ with} \\ X &= \left(\frac{\left(\frac{\alpha_2 \tan\,\varphi_0}{l\cos^3\,\theta_0} + 6b_1 t + 12b_2 t^2 + 20b_3 t^3\right)(2T^2)^2 l\cos^3\,\theta}{(2T(x_T - x_0) - T|x_T - x_0| + 2|x_T - x_0|t)^2}\right) \end{aligned} \tag{22}$$

Another method to calculate $v_2(t) = \dot{\varphi}$ is from Eq. (6) is:

$$\dot{\varphi} = \partial\left(l\frac{\ddot{y}\dot{x} - \ddot{x}\dot{y}}{r(\dot{x}^2 + \dot{y}^2)^{\frac{3}{2}}}\right)\left(\frac{1}{1 + \left(l\frac{\ddot{y}\dot{x} - \ddot{x}\dot{y}}{r(\dot{x}^2+\dot{y}^2)^{\frac{3}{2}}}\right)^2}\right) \tag{23}$$

Simulation parameters of a real vehicle are as follows: $l = 2\ m$, $r = 0.25\ m$, $x(0) = [0, 0, 0, 0]'$, $x(T) = \left[10, 10, 0, \frac{\pi}{6}\right]'$, and $T = 100$, the trajectory generation of this vehicle is generated from Eqs. (13) and (14). Vehicle velocity $v_1(t)$ is generated from Eqs. (19) or (20).

Body angle, θ, is from Eq. (13), and the angular velocity of body angle, $\dot{\theta}$, is from Eq. (21). The steering angle, φ, is from Eq. (14). The steering angular velocity, $\dot{\varphi}$, can be directly calculated form Eqs. (22) or (23). Figure 2 shows the coordinate trajectory (x, y) for the vehicle from initial position to the final position, and the velocity of the vehicle along the track. Figure 3 shows the vehicle body angle (θ), and the steering angle (φ), corresponding to the angular velocity ($\dot{\theta}$, $\dot{\varphi}$) of the vehicle.

From Fig. 3, the maximum steer angle for this movement, $\varphi_{\max} = 64°$, and exceed the physical constraint of a real vehicle with $-45° \le \varphi_{\max} \le 45°$. Therefore the above trajectory is not feasible. The problem is that the distance from the start point to the destination point is too short subject to the real vehicle physical constraints. A solution for this method is to lengthen the travelling distance until it meets the vehicle constraint on steer angle. This issue is discussed in the next section.

4 Trajectory Subject to Steer Angle Constraint

Due to a real structure constraint for a vehicle with $-\frac{\pi}{4} \le \varphi \le \frac{\pi}{4}$ or as mentioned above, the maximal angle for a real vehicle normally in a range of $-45° \le \varphi \le 45°$in the following constraint:

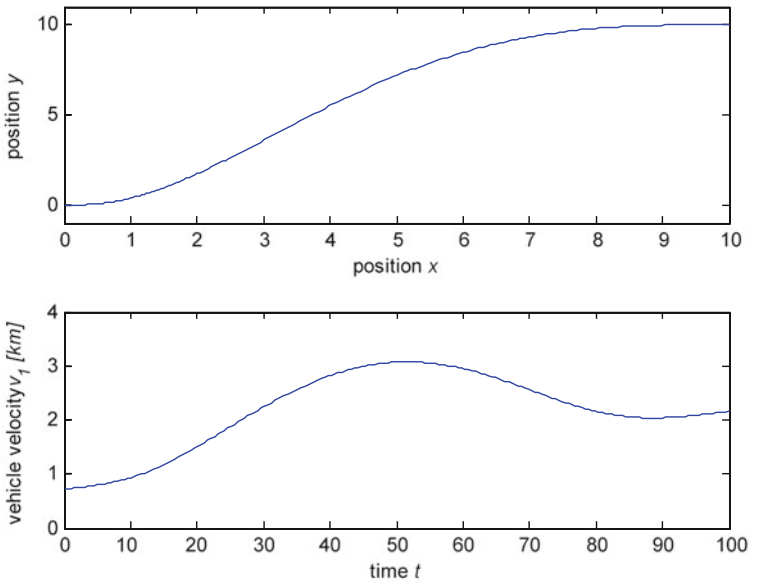

Fig. 2 Trajectory and velocity

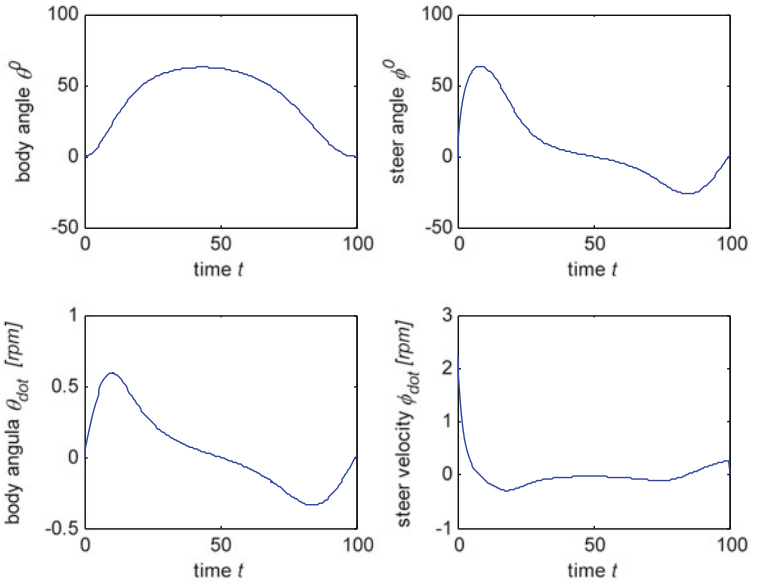

Fig. 3 Body and steer angle

$$-\frac{\pi}{4} \leq \varphi \leq \frac{\pi}{4} \tag{24}$$

Simulation in the previous part shows that the maximal needed steer angle, $\varphi_{\max} = 64^{\circ}$ and exceeds the requirement in (24). Therefore, in this part, a new method for the vehicle trajectory generation subject the constraint in Eq. (24) is proposed.

For time t from initial state, $t = 0$, to the final state, $t = T$, the feasible trajectory $x(t)$ and $y(t)$ subject to conditions in Eqs. (11) and (12) can be generated. For each progress of timing, t, re-calculate the steering angle, φ in Eq. (14), then, check for the steering constraint in Eq. (24). If the constraint in (24) is violated, it means that the distance from the initial position (x_0, y_0) to the final position (x_T, y_T) is too short for the steering angle.

In this case, this paper proposes to lengthen the distance $d_0 = \sqrt{(x_T - x_0)^2 + (y_T - y_0)^2}$ to a new distance with:

$$d_{Ni} = \rho^i d_0 \text{ with } \rho > 1 \tag{25}$$

for $i = 1, 2, 3, \ldots, n$ until the constraint in (24) is satisfied, and with ρ is an amplification coefficient, $\rho > 1$.

Then the new coordinates are:

$$x_{TN} = \rho^n (x_T - x_0), \text{ and } y_{TN} = \rho^n (y_T - y_0). \tag{26}$$

The next simulation is done with the same parameters in the previous part and subject to the constraint in Eq. (24) with an amplification coefficient $\rho = 1.1$. The constraint in (24) will be satisfied with $n = 4$ trials. The new coordinates are: $x_{TN} = y_{TN} = 23.579$.

Figure 4 shows the new trajectory and new velocity of the vehicle where the distance has been increased. The velocity of the vehicle is increased also since the final time T is not changed.

Figure 5 shows the new vehicle body angle (θ), velocity ($\dot{\theta}$) in rpm, steering angle (φ) and steering speed ($\dot{\varphi}$) in rpm for the new trajectory subject to the constraint of steer angle.

Due to the space limitations, the sideslip of this vehicle model is ignored in the present discussion. In reality, the sideslip of a vehicle depends on the tire stiffness and the cornering velocity. Then the trajectory generation of this study does not depend on the vehicle velocity. In the next part, a new vehicle trajectory generation based on polynomial distributions is investigated.

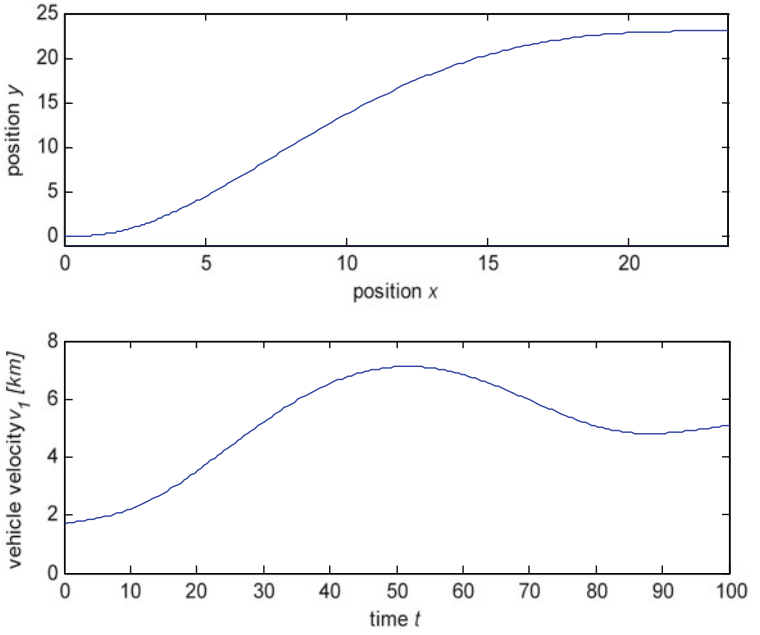

Fig. 4 Trajectory and velocity

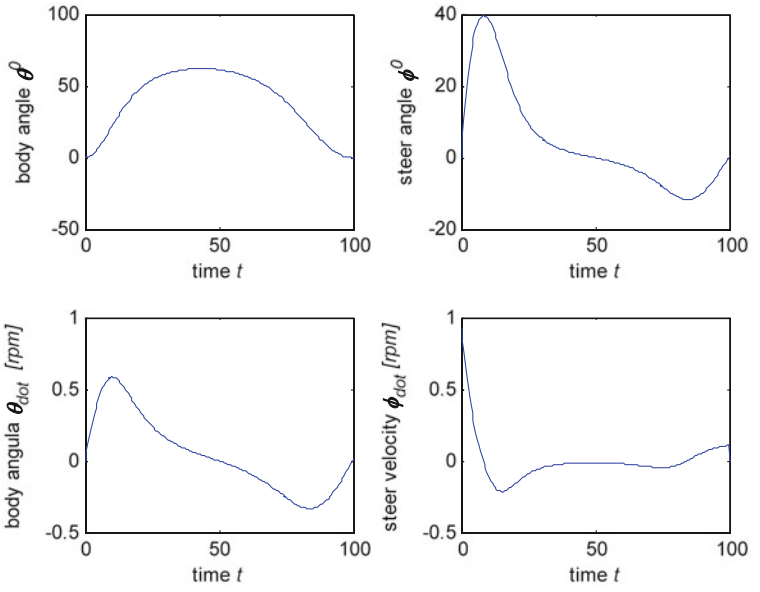

Fig. 5 Body and steer angle

5 Polynomial Trajectory Generation

For faster generation of a feasible vehicle tracking, Dong and Guo [3] have proposed a second order polynomial for flat output parameterizations. In order to do so, the Eq. (1) can be separated into the following forms:

$$z_1 = x,\ z_2 = \frac{\tan\ \varphi}{l\cos^3\ \theta},\ z_3 = \tan\ \theta \text{ and } z_4 = y \tag{27}$$

Then,

$$\dot{z}_1 = \dot{x} \tag{28}$$

$$\begin{aligned}\dot{z}_2 &= \frac{\dot{\varphi}\frac{1}{\cos^2\ \varphi} l\cos^3\ \theta + \dot{\theta} l 3\cos^2\ \theta \sin\ \theta \tan\ \varphi}{l^2\cos^6\theta} \\ &= \frac{v_2 l\cos^2\ \theta + 3rv_1\cos\ \theta\sin\ \theta\sin^2\ \varphi}{l^2\cos^5\ \theta\cos^2\ \varphi}\end{aligned} \tag{29}$$

$$\dot{z}_3 = \frac{\tan\ \varphi}{l\cos^2\ \theta} rv_1 \tag{30}$$

and

$$\dot{z}_4 = \dot{y} = \sin\ \theta rv_1 \tag{31}$$

The vehicle will move from the initial state (x_0, y_0, θ_0, φ_0) at time $t = 0$ to the final state (x_T, y_T, θ_T, φ_T) at time $t = T$ corresponding to the system in (27) from the initial state at ($z_{1.0}$, $z_{2.0}$, $z_{3.0}$, $z_{4.0}$) to the final state at ($z_{1.T}$, $z_{2.T}$, $z_{3.T}$, $z_{4.T}$).

For $0 \le t \le T$, the calculation of $[z_1(t), z_2(t), z_3(t), z_4(t)]$ will be:

$$z_1(t) = z_{1.0} + gt \tag{32}$$

$$z_2(t) = z_{2.0} + h_1 t + \frac{1}{2}h_2 t^2 + \frac{1}{3}h_3 t^3 \tag{33}$$

$$z_3(t) = z_{3.0} + gz_{2.0}t + \frac{1}{2}gh_1 t^2 + \frac{1}{6}gh_2 t^3 + \frac{1}{12}gh_3 t^4 \tag{34}$$

and

$$z_4(t) = z_{4.0} + gz_{3.0}t + \frac{1}{2}g^2 z_{2.0}t^2 + \frac{1}{6}g^2 h_1 t^3 + \frac{1}{24}g^2 h_2 t^4 + \frac{1}{60}g^2 h_3 t^5 \tag{35}$$

with, $g = \frac{z_{1.T} - z_{1.0}}{T}$, $[h_1, h_2, h_3]' = D^{-1}e$ $D = \begin{bmatrix} T & \frac{1}{2}T^2 & \frac{1}{3}T^3 \\ \frac{1}{2}gT^2 & \frac{1}{6}gT^3 & \frac{1}{12}gT^4 \\ \frac{1}{6}g^2T^3 & \frac{1}{24}g^2T^4 & \frac{1}{60}g^2T^5 \end{bmatrix}$ and

$$e = \begin{bmatrix} z_{2.T} - z_{2.0} \\ z_{3.T} - z_{3.0} - gz_{2.0}T \\ z_{4.T} - z_{4.0} - gz_{3.0}T - \frac{1}{2}g^2 z_{2.0}T^2 \end{bmatrix}.$$

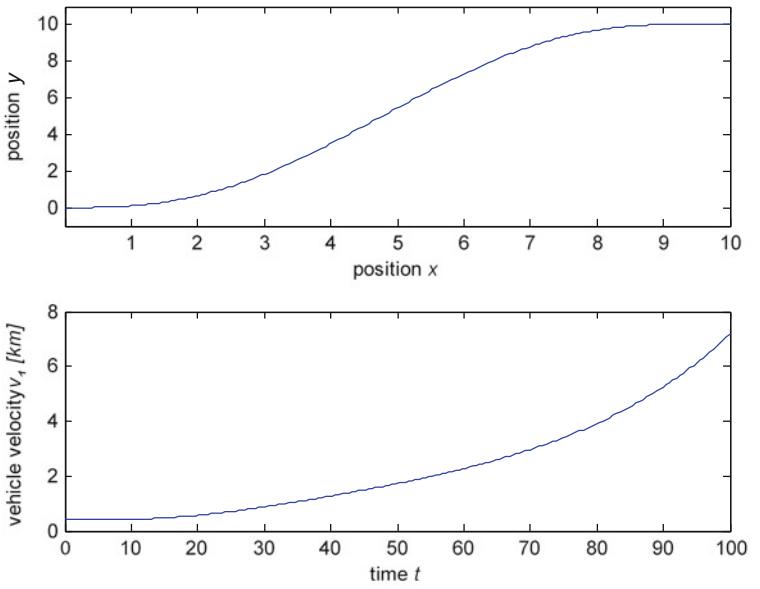

Fig. 6 Trajectory and velocity

Simulation of this trajectory generation is applied with the same parameters in Sect. 2 and shown in Figs. 6 and 7 using the following Eqs. from (36) to (42):

$$\theta = \arctan(z_3) \tag{36}$$

$$\varphi = \arctan(z_2 l \cos^3 \theta) \tag{37}$$

Putting,

$$\dot{x}(t) = \dot{z}_1(t) = g \tag{38}$$

$$\dot{y}(t) = \dot{z}_4(t) = g z_{3.0} + g^2 z_{2.0} t + \frac{1}{2} g^2 h_1 t^2 + \frac{1}{8} g^2 h_2 t^3 + \frac{1}{12} g^2 h_3 t^4 \tag{39}$$

Thus,

$$v_1(t) = \frac{\sqrt{\dot{x}^2(t) + \dot{y}^2(t)}}{r} \tag{40}$$

and

$$\dot{\theta} = \dot{z}_3 \cos^2 \theta = \left(g z_{2.0} + g h_1 t + \frac{1}{2} g h_2 t^2 + \frac{1}{3} g h_3 t^3 \right) \cos^2 \theta \tag{41}$$

and from Eq. (27)

$$\dot{\varphi} = \dot{z}_2(t) l \cos^3 \theta \cos^2 \varphi - 3\dot{\theta} \tan \theta \sin \varphi \cos \varphi \tag{42}$$

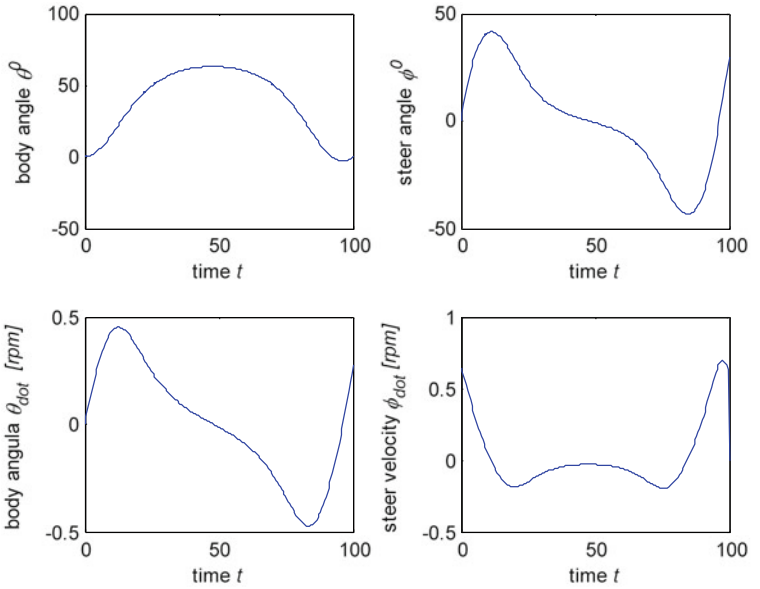

Fig. 7 Body and steer angle

Figure 6 shows the coordinate trajectory $(x,\ y)$ for the vehicle from initial point to the final point, and the velocity of the vehicle along the tracking.

Figure 7 shows the vehicle body angle,θ, and the steering angle, φ, corresponding to the angular velocity, $\dot{\theta}$, and, $\dot{\varphi}$, of the vehicle. The maximum steering angle for this trajectory generation is $\varphi = 41.5736°$ and satisfied the constraint on steering angle, $-45° \leq \varphi \leq 45°$. Therefore this trajectory generation is really better than the method presented in the previous part.From the vehicle velocity in Fig. 6, it is really not realistic to consider the vehicle speed increasing exponentially. In reality, when a vehicle is moving from one point to another point, it is better to assume that the speed will increase at the starting point and decrease at the destination point. Therefore, in the next part, a new symmetric polynomial with third order is investigated.

6 Symmetric Polynomial Trajectory Generation

Since the system is flatness and each flat output can be parameterized by a sufficiently smooth polynomials. In this part, a symmetric third order polynomial is tried for trajectory generation. Because the sideslip is ignored and then, the vehicle trajectory doesn't depend on the speed, v_1 or the travelling time, T, a new variable for this system regarding the travelling time is developed for $t = 0 \div T$:

$$x(t) = -(\frac{t}{T} - 1)^3 x_0 + \left(\frac{t}{T}\right)^3 x_T + a_x\left(\frac{t}{T}\right)^2(\frac{t}{T} - 1) + b_x\frac{t}{T}(\frac{t}{T} - 1)^2 \tag{43}$$

and the trajectory of y is:

$$y(t) = -(\frac{t}{T} - 1)^3 y_0 + \left(\frac{t}{T}\right)^3 x_T + a_y\left(\frac{t}{T}\right)^2(\frac{t}{T} - 1) + b_y\frac{t}{T}(\frac{t}{T} - 1)^2 \tag{44}$$

derivation of $x(t)$:

$$\dot{x}(t) = -3(\frac{t}{T} - 1)^2 x_0 + 3\left(\frac{t}{T}\right)^2 x_T + a_x 2\frac{t}{T}(\frac{t}{T} - 1) + a_x\left(\frac{t}{T}\right)^2 + b_x(\frac{t}{T} - 1)^2 + b_x 2\frac{t}{T}(\frac{t}{T} - 1) \tag{45}$$

and derivation of $y(t)$:

$$\dot{y}(t) = -3(\frac{t}{T} - 1)^2 y_0 + 3\left(\frac{t}{T}\right)^2 y_T + a_y 2\frac{t}{T}(\frac{t}{T} - 1) + a_y\left(\frac{t}{T}\right)^2 + b_y(\frac{t}{T} - 1)^2 + b_y 2\frac{t}{T}(\frac{t}{T} - 1) \tag{46}$$

Then,

$$\ddot{x}(t) = -6(\frac{t}{T} - 1)x_0 + 6\frac{t}{T}x_T + a_x 2(2\frac{t}{T} - 1) + a_x 2\frac{t}{T} + b_x 2(\frac{t}{T} - 1) + b_x 2(2\frac{t}{T} - 1) \tag{47}$$

and,

$$\ddot{y}(t) = -6(\frac{t}{T} - 1)y_0 + 6\frac{t}{T}y_T + a_y 2(2\frac{t}{T} - 1) + a_y 2\frac{t}{T} + b_y 2(\frac{t}{T} - 1) + b_y 2(2\frac{t}{T} - 1) \tag{48}$$

The constraint on speed:

$$rv_1 = \frac{\dot{x}}{\cos\,\theta} = \frac{\dot{y}}{\sin\,\theta} \tag{49}$$

The constraint at starting point $t = 0$:

$$\dot{x}(0) = k_0 \cos\,\theta_0, \text{ and } \dot{y}(0) = k_0 \sin\,\theta_0 \tag{50}$$

The constraint at destination point $t = T$:

$$\dot{x}(T) = k_T \cos\,\theta_T, \text{ and } \dot{y}(T) = k_T \sin\,\theta_T \tag{51}$$

From Eqs. (46), (47), (49) and (50), for the calculation simplicity, it is assumed that the speed coefficients at the start and destination point, $k_0 = k_T = k$, then

$$a_x = k\cos\,\theta_T - 3x_T, \text{ and } b_x = k\cos\,\theta_0 - 3x_0 \tag{52}$$

Similarly,

$$a_y = k \sin\ \theta_T - 3y_T, \text{ and } b_y = k \sin\ \theta_0 - 3y_0 \tag{53}$$

Simulation of this symmetric polynomial is conducted with the same parameters in the previous parts and shown in Figs. 8 and 9. The speed coefficients are $k_0 = k_T = k = 1$. Other parameters regarding the vehicle velocity, $v_1(t)$; the body angle, $\theta(t)$, and the body angle velocity, $\dot{\theta}(t)$; the steering angle, $\varphi(t)$, and the steering angle velocity, $\dot{\varphi}(t)$ are calculated in the following equations:

$$v_1 = \frac{\sqrt{\dot{x}^2 + \dot{y}^2}}{r} \tag{54}$$

$$\theta = \arctan\left(\frac{\dot{y}}{\dot{x}}\right) \tag{55}$$

$$\varphi = \arctan\left(l\frac{\cos^3\theta\ddot{y}}{(\dot{x})^2}\right) \text{ or } \varphi = \arctan\left(l\frac{\ddot{y}\dot{x} - \ddot{x}\dot{y}}{r(\dot{x}^2 + \dot{y}^2)^{\frac{3}{2}}}\right) \tag{56}$$

$$\dot{\theta} = \frac{\ddot{y}\dot{x} - \ddot{x}\dot{y}}{\dot{x}^2}\frac{1}{\left(\frac{\dot{y}}{\dot{x}}\right)^2 + 1} = \frac{\ddot{y}\dot{x} - \ddot{x}\dot{y}}{\dot{x}^2 + \dot{y}^2} = \frac{\tan\ \varphi}{l} r v_1 \tag{57}$$

and

$$\dot{\varphi} = \frac{\partial\left(\arctan\left(l\frac{\ddot{y}\dot{x} - \ddot{x}\dot{y}}{r(\dot{x}^2 + \dot{y}^2)^{\frac{3}{2}}}\right)\right)}{\partial t} \tag{58}$$

It can be seen from Fig. 8 that the trajectory of this symmetric polynomial is more realistic because the vehicle velocity increases from the starting point and decreases in the destination point.

As shown in Fig. 9, the maximum steering angle for this third order symmetric polynomial method is $\varphi = 41.1622°$ and satisfied the constraint on steering angle as $-45° \leq \varphi \leq 45°$. The steer angle is still a little bit smaller than the steer angle in the previous part for the second order polynomial method, $\varphi = 41.5736°$.

In the next part, an analysis and comparison of the above three methods are presented with simulations for the vehicles moving in both forward and backward directions.

7 Performance Analysis

Performance comparisons of the three methods on the trajectory generation and the vehicle velocity are shown in Figs. 10 and 11.

From Fig. 10, it can be seen that the polynomial method can produce a trajectory with smoother path. A symmetric polynomial generation can produce a

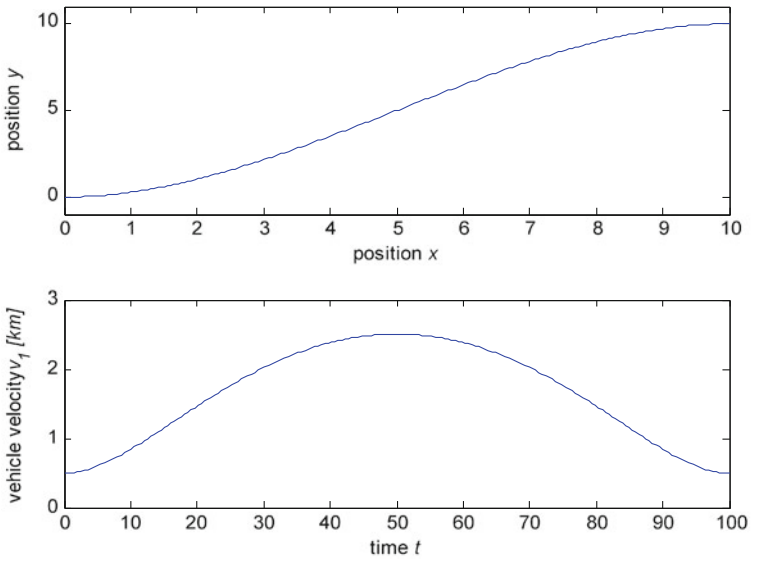

Fig. 8 Trajectory and velocity

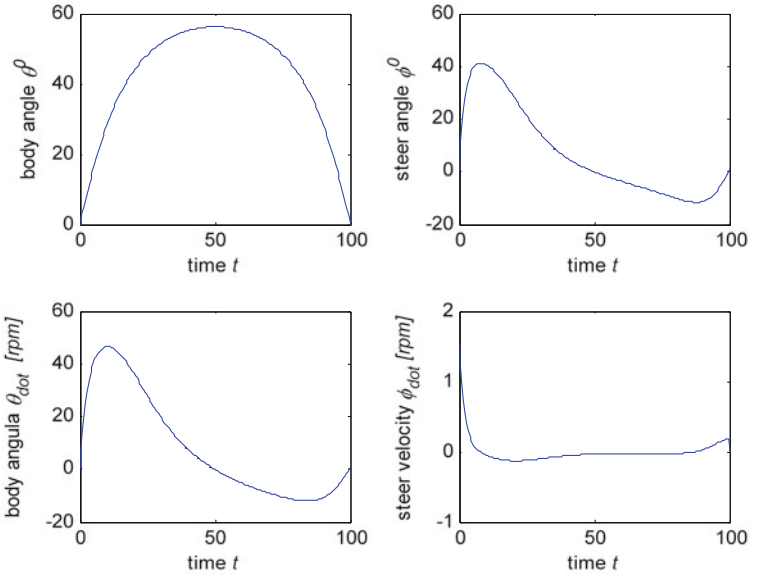

Fig. 9 Body and steer angle

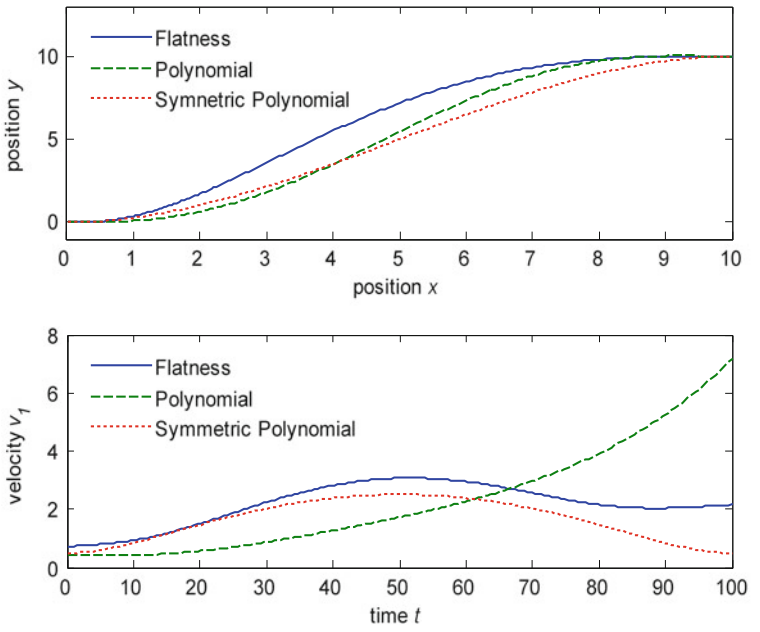

Fig. 10 Comparison of trajectory and velocity

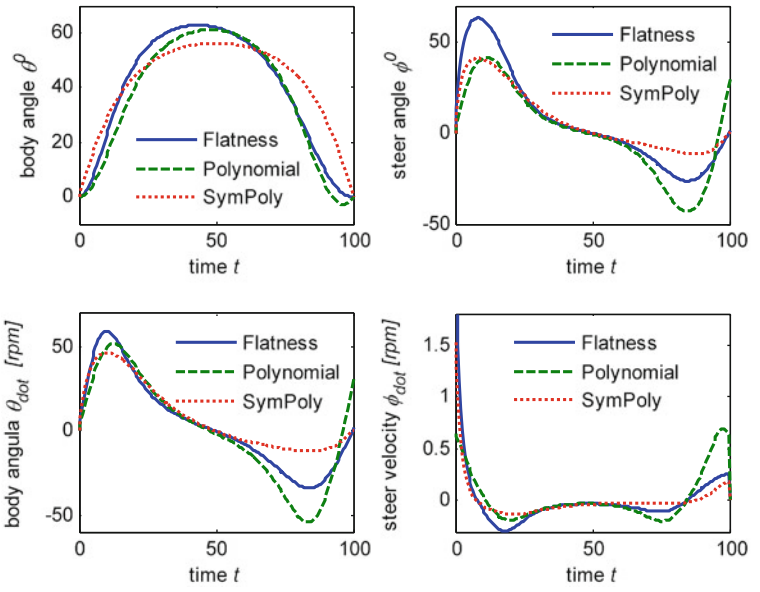

Fig. 11 Comparison of body and steer angle

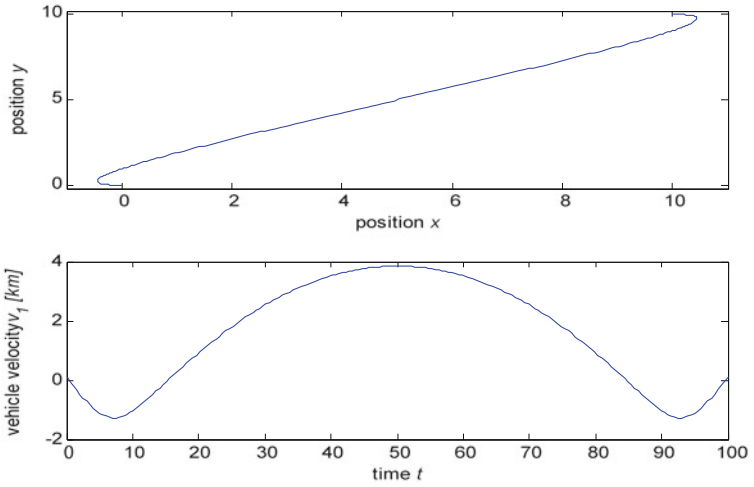

Fig. 12 Trajectory and velocity

more realistic speed since it allows the vehicle gradually increases the speed at the start point and reduces the speed at the destination point.

Figure 11 shows that the third order symmetric polynomial method can provide the lowest body angle, $\theta(t)$, the body angle velocity, $\dot{\theta}(t)$; the steering angle, $\varphi(t)$, and the steering angle velocity, $\dot{\varphi}(t)$. Then, this method is recommended for the development of an automatic control of tracking vehicles.

Studies for the vehicle moving in reverse speeds are also conducted. As mentioned in Eq. (3), the vehicle velocity, v_1, in reverse speeds will change the sign. Then the speed coefficients in Eqs. (52) and (53) will be minus values. Simulations for the vehicle in reverse speeds are done with the above third order symmetric polynomial trajectory generation. The speed coefficients now are assigned as, $k_0 = k_T = k = -1$. Results of the simulation are shown in Figs. 12 and 13.

Since the vehicle is forced to reverse at the start point, for $k_0 = -1$, and at the destination point, for $k_T - 1$, Fig. 12 shows the vehicle backing out at the start point, going forward to the destination, then backing to the destination parking space. The vehicle velocities are changing the direction in three times.

Figure 13 shows the body angle, θ, switching 180° in two times corresponding to each reverse speeds. The maximum steering angle in this reverse trajectory is, $\varphi_{\max} = 33.7097°$, and much lower than the required angles in forward movements. The body angular velocity, $\dot{\theta}$, as well as the steering angular velocity, $\dot{\varphi}$, are also indicated during this reverse performance.

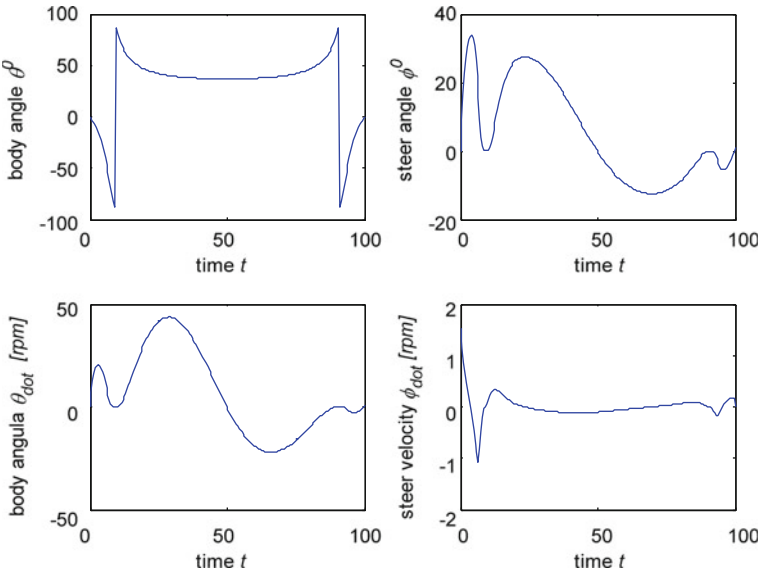

Fig. 13 Body and steer angle

8 Conclusion

The chapter has presented three methods of trajectory generation for autonomous vehicles subject to constraints. Regarding to the real vehicle speed development, the third order symmetric polynomial trajectories are recommended. Simulations and analyses are also conducted for vehicle with forward and reverse speeds. Results from this study can help to develop a real-time control system for auto-driving and auto-parking vehicles. The limitation of this study is to ignore the influence of the vehicle sideslip due to the cornering velocity. However this error can be eliminated with the feedback control loop and the offset margin of the steer angle allowance.

References

1. J. Choi, R. Curry, G. Elkaim, Curvature-Continous trajectory generation with corridor constraint for automomous ground vehicles, in *Proceedings of IEEE Conference of Decision and Control*, Atlanta, Georgia, 15–17 Dec 2010
2. V. Delsart, T. Fraichard, L. Martiez, Real-Time trajectory generation for car-like vehicles navigating dynamic environments,in *proceedings of IEEE International Conference on Robotics and Automation*, Kobe, Japan, 12–17 May 2009
3. W. Dong, Y. Guo, New trajectory generation methods for nonholonomic mobile robots, in *Proceedings of the International Symposium on Collaborative Technologies and Systems*, Missouri, USA, 20–20 May 2005

4. M. Gomez, Optimal control for wheeled mobile vehicles based on cell mapping techniques, in *Proceedings of IEEE Intelligent Vehicles Symposium,* Eindhoven, Netherland, 4–6 June 2008
5. K. Kanjanawanishkul, M. Hofmeister, A. Zell, Smooth reference tracking of a mobile robot using nonlinear model predictive control, in *Proceedings of the 4th European Conference on Mobile Robots,* Mlini/Dubrovnik, Croatia, 23–25 Sept 2009
6. G. Klancar, Tracking-error model-based predictive control for mobile robots in real time. Robot. Auton. Syst. **55**(6), 460–469 (2007)
7. J. Levine, *Analysis and control of nonlinear system, a flatness-based approach* (Springer, Heidelberg, 2009)
8. VT. Minh, Vehicle steering dynamic calculation and simulation, in *Proceedings of the 23rd International DAAAM Symposium on Intelligent Manufacturing and Automation*, Zadar, Croatia, 24–27 Oct 2012
9. V.T. Minh, Stabillity for switched dynamic hybrid systems. Math. Comput. Modell. **57**(1–2), 78–83 (2013)
10. V.T. Minh, H. Fakhruldin, Time forward observer based adaptive controller for a teleoperation system. Int. J. Control Autom. Syst. **9**(3), 470–477 (2011)
11. V.T. Minh, A. Nitin, A comparative study on computational schemes for nonlinear model predictive control. Asian. J. Control. **8**(4), 324–331 (2006)
12. M. Missura, S. Behnke, Efficient kinodynamic trajectory generation for wheeled robots, in *Proceedings of IEEE International Conference on Robotics and Automation*, Shanghai, China, 9–13 May 2011
13. J. Wang, Z. Lu, W. Chen et al, An adaptive trajectory tracking control of wheeled mobile robots, in *Proceedings of IEEE Conference on Industrial Electronics and Applications*, Beijing, China, 21–23 June 2011
14. M. Werling, S. Kammel, J. Ziegler et al., Optimal trajectories for time-critical street scenarios using discretized terminal manifolds. Int. J. Robot. Res. **31**(3), 346–359 (2011)
15. T. Zhou, M. Li, Z. Mai et al, Trajectory generation model-based IMM tracking for safe driving in intersection scenario. Int. J. Veh. Technol.(2011). doi:10.1155/2011/103696